Published in final edited form as:
Biomaterials. 2010 July ; 31(21): 5536–5544. doi:10.1016/j.biomaterials.2010.03.064.

Cell-laden microengineered gelatin methacrylate hydrogels

Jason W. Nichol[1,2,†], **Sandeep Koshy**[1,2,3,†], **Hojae Bae**[1,2,†], **Chang Mo Hwang**[1,2], **Seda Yamanlar**[1,2], and **Ali Khademhosseini**[1,2,*]

[1] Center for Biomedical Engineering, Department of Medicine, Brigham and Women's Hospital, Harvard Medical School, 65 Landsdowne Street, Cambridge, MA 02139, USA

[2] Harvard-MIT Division of Health Sciences and Technology, Massachusetts Institute of Technology, Cambridge, MA 02139, USA

[3] Department of Chemical Engineering, University of Waterloo, Waterloo, ON, N2L 3G1, Canada

Abstract

The cellular microenvironment plays an integral role in improving the function of microengineered tissues. Control of the microarchitecture in engineered tissues can be achieved through photopatterning of cell-laden hydrogels. However, despite high pattern fidelity of photopolymerizable hydrogels, many such materials are not cell-responsive and have limited biodegradability. Here we demonstrate gelatin methacrylate (GelMA) as an inexpensive, cell-responsive hydrogel platform for creating cell-laden microtissues and microfluidic devices. Cells readily bound to, proliferated, elongated and migrated both when seeded on micropatterned GelMA substrates as well as when encapsulated in microfabricated GelMA hydrogels. The hydration and mechanical properties of GelMA were demonstrated to be tunable for various applications through modification to the methacrylation degree and gel concentration. Pattern fidelity and resolution of GelMA was high and it could be patterned to create perfusable microfluidic channels. Furthermore, GelMA micropatterns could be used to create cellular micropatterns for in vitro cell studies or 3D microtissue fabrication. These data suggest that GelMA hydrogels could be useful for creating complex, cell-responsive microtissues, such as endothelialized microvasculature, or for other applications that requires cell-responsive microengineered hydrogels.

Keywords

tissue engineering; hydrogel; gelatin; photopolymerisation; micropatterning

Introduction

The cellular microenvironment plays a critical role in controlling cell behavior and function [1]. Recent work has been directed towards controlling the microenvironment to investigate morphologically mediated cell behaviors such as cell shape [2,3], cell-cell contacts, and signaling [4,5]. As specific microarchitectural features of the cell niche and the micromechanical environment have been demonstrated to be vital to controlling cell

[*]Correspondence should be addressed to Ali Khademhosseini (alik@rics.bwh.harvard.edu), 65 Landsdowne Street, Cambridge, MA 02139, USA.
[†]Jason W. Nichol, Sandeep Koshy, and Hojae Bae contributed equally to this work.

differentiation [6–9], researchers have sought materials with improved biological, chemical and mechanical properties.

The emerging field of microscale tissue engineering [1,10] investigates incorporating precise control over cellular microenvironmental factors, such as microarchitecture, in engineered tissues with the ultimate goal of directing cell and tissue function. In many tissues, such as the lobule of the liver [11], cells exist in complex, functional units with specific cell-cell and cell-extracellular matrix (ECM) arrangements that are repeated throughout the tissue. Therefore, creation and characterization of these functional units may be beneficial in engineering tissues. Tissue modules [12] can be made to generate macroscale tissues from microscale functional units made of cell-seeded [13,14] or cell-laden [11,15–17] hydrogels. Typically, creation of these microscale hydrogels, or microgels, is achieved by using micromolding [18] or photopatterning [15] techniques yielding cell-laden constructs with specific microarchitectural features matching the desired tissue. For these applications it is vital not only to match the morphology of the functional units, but also the cellular arrangement, making control of hydrogel properties, such as mechanical stiffness, cell binding and migration, critical to proper cellular function and tissue morphogenesis.

Many successful applications of microscale tissue engineering have demonstrated tight control of co-culture conditions and cell-cell interactions [11,15]. However, many of the currently available hydrogels suffer from poor mechanical properties, cell binding and viability or the inability to control the microarchitecture. Native ECM molecules, such as collagen, can be used to create cell-laden microgels, however the ability to create lasting micropatterns is limited typically due to insufficient mechanical robustness. Conversely, while some hydrogels, such as polyethylene glycol (PEG) [15,17] or hyaluronic acid (HA) [17,19], can have stronger mechanical properties and excellent encapsulated cell viability, cells typically cannot bind to, nor significantly degrade these materials. This lack of cell responsive features greatly limits the ability of the cells to proliferate, elongate, migrate and organize into higher order structures. Addition of the binding sequence Arg-Gly-Asp (RGD) [20–22], or incorporating interpenetrating networks of ECM components [19], has been shown to improve cell binding and spreading, however, without the ability for cells to degrade the hydrogel, cell movement and organization in 3D could be limited. New formulations of PEG, containing incorporated RGD and matrix metalloproteinase (MMP)-sensitive degradation sequences [23–26], have shown great promise in a variety of applications, however they have not been widely used in microscale tissue engineering.

Gelatin methacrylate (GelMA) is a photopolymerizable hydrogel comprised of modified natural ECM components [27], making it a potentially attractive material for tissue engineering applications. Gelatin is inexpensive, denatured collagen that can be derived from a variety of sources, while retaining natural cell binding motifs, such as RGD, as well as MMP-sensitive degradation sites [28,29]. Addition of methacrylate groups to the amine-containing side groups of gelatin can be used to make it light polymerizable into a hydrogel that is stable at 37 °C. Long-term cell viability, and limited encapsulated cell elongation, have been demonstrated [30], however many key physical and cell-responsive properties of GelMA are not well studied. In addition, GelMA has not been used in microscale applications making its suitability for this purpose uncertain.

We hypothesized that as a light polymerizable hydrogel based on collagen motifs, GelMA could successfully be micropatterned into a variety of shapes and configurations for tissue engineering and microfluidic applications, while retaining its high encapsulated cell viability and cell-responsive elements (binding, degradation). In this report, we investigated the surface and 3D cell binding, cell elongation and migration properties of GelMA microgels. In addition,

we investigated whether cell-laden GelMA could be made into perfusable microchannels which could be seeded with endothelial cells, for creating perfusable engineered tissues.

Materials and Methods

Materials

Polyethylene glycol diacrylate (PEGDA), gelatin (Type A, 300 bloom from porcine skin), methacrylic anhydride (MA) and 3-(trimethoxysilyl)propyl methacrylate (TMSPMA) were purchased from Sigma-Aldrich (Wisconsin, USA). Glass slides and coverslips were purchased from Fisher Scientific (Philadelphia, USA). Printed photomasks were purchased from CADart (Washington, USA), while the UV light source used (Omnicure S2000) was manufactured at EXFO Photonic Solutions Inc. (Ontario, Canada). Spacer thickness was measured with electronic digital micrometer calipers (Marathon Watch Company Ltd, Ontario, Canada).

Methacrylated gelatin synthesis

Methacrylated gelatin was synthesized as described previously [27] (Figure 1A). Briefly, type A porcine skin gelatin was mixed at 10% (w/v) into Dulbecco's phosphate buffered saline (DPBS; GIBCO) at 60°C and stirred until fully dissolved. MA was added until the target volume was reached at a rate of 0.5 mL/min to the gelatin solution under stirred conditions at 50 °C and allowed to react for 1 h. The fraction of lysine groups reacted was modified by varying the amount of MA present in the initial reaction mixture. Following a 5X dilution with additional warm (40 °C) DPBS to stop the reaction, the mixture was dialyzed against distilled water using 12–14 kDa cutoff dialysis tubing for 1 week at 40 °C to remove salts and methacrylic acid. The solution was lyophilized for 1 week to generate a white porous foam and stored at −80 °C until further use.

^{1}H NMR

The degree of methacrylation was quantified by using the Habeeb method [30,31] and ^{1}H-NMR from a method previously described for methacrylate modified collagen [32]. The composition of acid treated porcine skin gelatin used for analysis of ^{1}H-NMR data was acquired from previously published data [33]. ^{1}H-NMR spectra were collected at 35 °C in deuterium oxide (Sigma) at a frequency of 500 MHz using a Varian INOVA NMR spectrometer with a single axis gradient inverse probe. Three spectra were collected from each sample. Solvent presaturation was employed to suppress the large HOD signal. Phase correction was applied to obtain purely absorptive peaks. Baseline correction was applied before obtaining the areas (integrals) of the peaks of interest.

Hydrogel preparation and characterization

Freeze dried GelMA macromer was mixed into DPBS containing 0.5% (w/v) 2-hydroxy-1-(4-(hydroxyethoxy)phenyl)-2-methyl-1-propanone (Irgacure 2959, CIBA Chemicals) as a photoinitiator at 80 °C until fully dissolved.

Mechanical testing

Two hundred microliters of prepolymer was pipetted between two glass coverslips separated by a 750 μm spacer and exposed to 6.9 mW/cm^2 UV light (360–480 nm) for 60 s (Figure 1B). Samples were detached from the slide and incubated free floating at 37 °C in DPBS for 24 h. Immediately prior to testing, an 8 mm disc was punched from each swollen hydrogel sheet using a biopsy punch. The disc was blotted lightly with a KimWipe and tested at a rate of 20% strain/min on an Instron 5542 mechanical tester. The compressive modulus was determined as the slope of the linear region corresponding with 0–5% strain.

Hydrogel swelling analysis

Polymerization was performed as described for mechanical testing. Immediately following hydrogel formation, an 8 mm radius disc of each composition was punched from a flat thin sheet and placed in DPBS at 37 °C for 24 h. Discs were removed from DPBS and blotted with a KimWipe to remove the residual liquid and the swollen weight was recorded. Samples were then lyophilized and weighed once more to determine the dry weight of polymer. The mass swelling ratio was then calculated as the ratio of swollen hydrogel mass to the mass of dry polymer.

Cell culture

Immortalized human umbilical vein endothelial cells (HUVEC; a generous gift from Dr. J. Folkman, Children's Hospital, Boston) constitutively expressing green fluorescent protein (GFP) were maintained in endothelial basal medium (EBM-2; Lonza) and supplemented with endothelial growth BulletKit (Lonza) in a 5% CO_2 atmosphere at 37 °C. Cells were passaged approximately 2 times per week and media was exchanged every 2 days. NIH 3T3 fibroblasts were maintained in DMEM supplemented with 10% FBS and passaged 2 times per week.

Cell Adhesion

For cell adhesion studies, square hydrogel sheets (1 cm (w) × 1 cm (l) × 750 μm (h)) were prepared in a similar manner as that used for mechanical testing onto TMSPMA glass slides. Slides were covered with a HUVEC suspension containing 2.5×10^5 cells/mL to a depth of approximately 1 mm above the surface of the GelMA hydrogel and incubated for 12 h prior to washing twice with DPBS. Media was changed every 12 h for 5 days. GFP fluorescence was visualized using an inverted fluorescence microscope (Nikon TE 2000-U) equipped with a GFP filter cube. GFP images were used to quantify total cell area using NIH ImageJ software. After 5 days, cells were fixed and stained with rhodamine-phalloidin (Invitrogen) and DAPI to visualize F-actin filaments and cell nuclei respectively. Total cell number was quantified using ImageJ by counting DAPI stained nuclei.

Cell encapsulation

NIH 3T3 fibroblasts were trypsinized and resuspended in GelMA macromer containing 0.5% (w/v) photoinitiator at a concentration of 5×10^6 cells/mL. Microgel units (500 μm × 500 μm) were fabricated as previously described [15] following exposure to 6.9 mW/cm^2 UV light (360–480 nm) for 15 s on TMSPMA treated glass. The glass slides containing microgels were washed with DPBS and incubated for 8 h in 3T3 medium under standard culture conditions. A calcein-AM/ethidium homodimer Live/Dead assay (Invitrogen) was used to quantify cell viability within the microgels according to the manufacturer's instructions.

Selectively adhesive arrays

To generate selectively adhesive hydrogel arrays, a composite structure of PEG dimethacrylate and GelMA was fabricated. A 10 μL drop of 20% (w/v) PEG (MW: 4000) prepolymer mixture consisting of 1% (w/v) photoinitiator was placed between a TMSPMA coated slide and an untreated coverslip (18 mm (w) × 18 mm (l)) and exposed to 6.9 mW/cm^2 UV light (360–480 nm) for 15 s. After removal of the untreated slide the PEG layer was washed and immersed in DPBS for 15 minutes. GelMA microgel units (500 μm × 500 μm, 10% (w/v), 0.5% (w/v) photoinitiator) were fabricated using a procedure as previously described for PEGDA [15] with exposure to 6.9 mW/cm^2 UV light (360–480 nm) for 15 s. The arrays were incubated for 12 h at 37 °C in DPBS to remove excess uncrosslinked gelatin which may be lightly adhered to the PEG layer. A HUVEC suspension (2×10^6 cells/mL) was added on top of the PEG/GelMA to a depth of approximately 1 mm and cultured for 12 h, washed twice with DPBS and further

incubated for 12 h. Cells bound to GelMA micropatterns were imaged after treatment with calcein-AM following an additional 12 h of culture in fresh media.

Microvascular channel creation and perfusion

To create perfusable microchannels 200 μL of 15% (w/v) GelMA (1% (w/v) photoinitiator) containing 5×10^6 cells/mL was poured within a rectangular PDMS mold (~1 cm × 0.3 cm) containing a 30 gauge needle placed atop of 300 μL spacers on a standard glass slide. The macromer-filled mold was exposed to 6.9 mW/cm^2 UV light (360–480 nm) for 30 s on each side to assure even polymerization. The rectangular GelMA block was then removed from the mold and the needle was gently withdrawn. Entrance and exit ports were created using a 3 mm diameter disposable biopsy punch for the introduction of inlet and outlet tubing to enable perfusion. Initial perfusion studies were performed by using 2000 kDa FITC-dextran. For cell perfusion experiments, a 5 μL drop of 2×10^6 cells/mL HUVEC was applied to the entrance of the channel and drawn in by capillary force. Microchannels were immersed in media and placed at standard cell culture conditions. To visualize, 3T3 cells were stained with PKH67 according to the manufacturer's instructions (Sigma).

Statistics

Data were compared using ANOVA followed by Bonferroni's post-hoc test GraphPad Prism 5.00 (GraphPad Software, San Diego, USA).

Results

Determination of degree of methacrylation

GelMA was synthesized using various concentrations of MA to create polymers with different degrees of methacrylation. To quantify the differences between samples, the Habeeb assay was used to determine the extent of substitution of free amine groups in gelatin samples, as the methacrylate groups only bound to free amine groups. The number of methacrylate groups was also directly verified by ^{1}H-NMR with close agreement (Figure 2). These results demonstrated the ability to create GelMA polymers with a degree of methacrylation varying roughly from 20% to 80% (Figure 2). Three batches of GelMA were created with "high" (81.4 ± 0.4%), "medium" (53.8 ± 0.5%) and "low" (19.7 ± 0.7%) methacrylation degree corresponding to 20%, 1.25%, and 0.25% volume percentage MA added to the synthesis reaction respectively, and were used in the remainder of the experiments.

Mechanical properties

Mechanical properties of the matrix environment have been shown to affect cell function and differentiation [7,8]. To determine the effect of methacrylation degree and gel concentration on the mechanical properties of the GelMA hydrogels, unconfined compression was performed on samples with high, medium, and low methacrylation degree at GelMA concentrations of 5%, 10%, and 15%. In general, increasing the degree of methacrylation increased the stiffness at all strain levels for all three gel percentages as demonstrated in the representative curve for the 15% (w/v) GelMA cases (Figure 3A). The compressive modulus was significantly higher for low, medium, and high degrees of methacrylation at both the 15% and 10% (w/v) GelMA concentrations (Figure 3B). This behavior was consistent at the 5% (w/v) GelMA concentration, however the difference was not statistically significant. Similarly, maintaining a constant degree of methacrylation while increasing the GelMA concentration significantly increased the compressive modulus under all conditions tested. No sample failed before the maximum 50 N load was reached, demonstrating the elastomeric properties of the GelMA under all conditions. The 5% (w/v) GelMA with a low degree of methacrylation formed a weak gel upon polymerization and could not be tested.

Swelling characteristics

The swelling characteristics of a network are important in various applications as it affects solute diffusion, surface properties, mechanical properties, and surface mobility [34]. The degree of swelling of gels is dependent on the pore size of the polymer network and the interaction between the polymer and the solvent [15]. As hydration can have a substantial effect on the physical properties of the resultant hydrogel and fidelity of the desired micropattern, the change in mass swelling ratio of GelMA was investigated relative to the hydrogel concentration and degree of methacrylation. Hydrogels were made as described previously at 5%, 10%, or 15% (w/v) GelMA of low, medium, or high degree of methacrylation. Hydrogels were allowed to reach equilibrium over a 24 h incubation in DPBS at room temperature, then the mass swelling ratio of the swollen mass to the dry mass of polymer was calculated and compared (Figure 5). Holding the hydrogel percentage constant, the mass swelling ratio increased significantly with decreasing degree of methacrylation at all three hydrogel concentrations, demonstrating that the degree of methacrylation had a significant effect on the material's ability, and propensity, for attracting and storing water within the polymer network. Conversely, holding the methacrylation degree constant and decreasing the macromer concentration increased the mass swelling ratio in all cases with nearly all differences being significant. As swelling can have a profound effect on the overall shape of patterned hydrogels, especially when micro/nano patterned in intricate shapes, this data suggests that pattern fidelity would be improved by increasing the degree of methacrylation, hydrogel percentage, or both.

Cell adhesion to 2D GelMA surfaces

The ability to bind to scaffold materials is essential for cell survival and function in engineered tissues [10]. Therefore the surface adhesion characteristics of GelMA were determined at 5%, 10%, and 15% (w/v) GelMA concentration at the high degree of methacrylation (Figure 5). The high degree of methacrylation was chosen as this formulation performed best in micropatterning applications, the low degree formed weak gels that could not be handled at 5% (w/v), and in preliminary studies GelMA with a medium degree of methacrylation behaved similarly to the high degree (data not shown). HUVECs were chosen as a model cell type for the potential application of GelMA in vascularized tissue engineering as well as to explore the compatibility of GelMA with a human cell type. HUVEC readily bound to GelMA surfaces of all concentrations with roughly the same affinity following initial seeding. There were no significant differences in the cell number, as determined by the percentage of confluency, within the first 24 hours. Cells on GelMA surfaces of all concentrations elongated, migrated, and aggregated with surrounding cells forming branched and interconnected multicellular networks by day 2. GelMA of 5% (w/v) macromer concentration demonstrated a decreased confluency as compared to 10% and 15% (w/v) being significantly different from both on day 3. Both 10% and 15% (w/v) GelMA demonstrated significantly increased confluency over 5 days, increasing at least 2 to 3 fold in the given time. Significant differences in overall confluency between 10% and 15% (w/v) GelMA concentration were seen by day 5. Similar significant differences in the cell density, defined as the number of DAPI positive cells per fixed area, demonstrated that cell density significantly increased with increased GelMA concentration. This suggests that the relationship between confluency and hydrogel concentration was not solely due to increased cell spreading.

The overall cellular morphology appeared to be largely single cell-width networks with 5% (w/v) GelMA, with the overall width of cell aggregates increasing with GelMA percentage. Combined with the quantified cell density and confluency data, this suggests that the difference in morphology is, at least in part, due to increased cell number and aggregation, rather than increased cell spreading or increased cell size. These differences in cell behavior are likely due to a combination of variations in the stiffness of the GelMA surfaces relative to the gel concentration, and increases in the density of bioactive sequences with increased macromer

concentration. Lumen-like ring structures were apparent at all GelMA concentrations, suggesting maintenance of endothelial phenotype. As expected, few cells adhered to PEGDA 4000 surfaces, as PEG is not cell adhesive, and the confluency was observed to decrease over time.

3D cell encapsulation in GelMA micropatterns

To successfully employ micropatterned GelMA as a hydrogel suitable for tissue engineering applications, encapsulated cell behavior was investigated within micropatterned, high degree of methacrylation GelMA. In initial experiments using basic square patterns with feature size as small as 100 μm, GelMA performed similarly to PEG in terms of pattern fidelity and short exposure time suggesting that cell viability properties would be similar to that of PEG (data not shown). NIH 3T3 fibroblasts were (w) × 500 μm (l) × 300 μm (h) GelMA micropatterns at concentrations of 5%, 10%, and 15% (w/v). All conditions yielded high pattern fidelity and initial cell viability demonstrating GelMA's high potential for use as a cell-laden hydrogel for microscale tissue engineering applications (Figure 6A–C). Viability 8 h after encapsulation was 92 ± 2% in 5% GelMA, which was significantly higher than that in 10% (82 ± 2%) or 15% (75± 4%) (w/v) GelMA microgel samples ($p < 0.05$). Cell viability has previously been shown to decrease with macromer concentration in other hydrogel systems [15, 18]. General losses in viability may occur due to encapsulation stress, nutrient limitations, drying during processing or stress due to transient swelling after placement in media. It is expected that with further optimization of photoinitiator concentration and UV exposure duration, higher initial viabilities could be produced. Initial viability was similar to that determined in bulk hydrogels, demonstrating that micropatterning did not significantly alter cell viability properties more than UV polymerization alone. Long term viability (up to 15 days) in bulk GelMA was similar to the viability measured at early time points as published previously, demonstrating that the polymerization and patterning conditions did not adversely affect cell viability in the short or long term [30].

After 3 days in culture, cells readily elongated in all three GelMA percentages, with elongation and migration varying inversely with gel concentration (Figure 6D–F). In 5% (w/v) gels, cells elongated, migrated and formed interconnected networks with neighboring cells, in addition to contracting and degrading the micropatterned GelMA to extravasate onto the glass slide. Cells did not migrate or degrade the microgels to the same extent in 10% or 15% (w/v), however individual elongated cells and small, multicellular networks could be seen in both groups demonstrating that while increased hydrogel concentration may slow the process, it is not inhibited entirely.

Selective adhesion onto micropatterned GelMA surfaces

To demonstrate the feasibility of using GelMA for selective cell seeding and controlled co-culture environments for tissue engineering applications, adhesion of cells 500 μm (l) × 300 μm (h) μm GelMA patterns were prepared as described previously on the surface of a PEGDA 4000 layer which was first polymerized onto the glass slide surface to inhibit cell adhesion except on the GelMA surfaces. Therefore, the GelMA micropatterns were polymerized onto the PEG surface directly, which was performed with little difficulty as compared to creating GelMA micropatterns directly on glass slides. The GelMA microgels were observed to adhere robustly to the PEGDA surface, suggesting covalent bonding between the two materials, which is suitable for generating stable composite micropatterned structures. Following GelMA micropattern fabrication and incubation in DPBS to remove uncrosslinked gelatin from PEG surfaces, HUVEC cells (2×10^6 cells/mL) were pipetted onto the surface and incubated for 12 h to allow for adhesion to occur, washed with DPBS to remove non-adherent cells, then incubated for an additional 12 h to demonstrate persistence. As demonstrated, HUVEC cells

bound only to GelMA surfaces, and not to PEG surfaces, quickly creating a confluent monolayer on GelMA patterns (Figure 7).

Microfluidic channels with endothelial linings created in GelMA

To demonstrate the use of GelMA in microfluidic systems, and as a potential biomaterial for producing vascularized engineered tissues, endothelial cells were seeded into a perfusable GelMA microchannel. For these tests, a block of GelMA was polymerized containing a syringe needle, which when removed contained a 300 μm diameter perfusable channel (Figure 8A). Rhodamine-labeled 3T3 fibroblasts were embedded within the GelMA bulk, while FITC-Dextran (2000 kDa) was perfused through the microchannel to demonstrate the ability to create perfusable, microfluidic channels within cell-laden GelMA structures (Figure 8B–C). To investigate the ability to create cell-laden constructs with endothelial-lined microchannels, HUVEC cells were seeded into the channel and allowed to adhere (Figure 8D). The resultant co-cultured construct of 3T3 cells with a HUVEC-lined microchannel demonstrate the potential for making co-cultured, engineered constructs with perfusable microvasculature networks.

Discussion

Gelatin is created through either acid or alkaline hydrolysis of collagen, and has long been employed for pharmaceutical, food, and cosmetic products. The alkaline hydrolysis process hydrolyzes the amide structures of asparagine or glutamine side chains generating a high percentage of carboxylic groups [35] therefore increasing the isoelectric point to 9, whereas acidic hydrolysis leads to an isoelectric point of 5 [36]. Depending on the isoelectric point, gelatin could bind different types of growth factors and also promote the proliferation of various cell types [37,38]. In addition, the chemical functionalities present in gelatin (carboxylic acid, thiol, hydroxyl) allows for potential covalent modification of the GelMA with growth factors or cytokines to further promote cell viability and function. Therefore, GelMA could potentially be tailored to different cell or tissue types, or growth factor and drug delivery applications, based on the specific type of gelatin precursor selected.

Crosslinking of gelatin by different methods has been utilized to create gelatin hydrogels that are stable at physiological temperatures (37 °C), more resistant to degradation by proteolytic enzymes such as gelatinase and collagenases [35], and mechanically robust [39,40]. Chemical crosslinking agents such as glutaraldehyde, carbodiimide, diphenylphosphoryl azide and enzymatic crosslinkers, such as microbial transglutaminase (mTG), have been used to crosslink gelatin [41–43], however, these crosslinking agents are often cytotoxic or elicit immunological responses from the host [41,42,44–48]. Moreover, these chemical or enzymatic crosslinking methods do not support 3D encapsulation of viable cells, making them ill suited for creating cell-laden microgels.

Enhancing the ability of cells to elongate, migrate, and connect with neighboring cells in 3D is vital to recreating native tissue morphology in engineered tissues. Encapsulating cells in hydrogels such as PEG and HA allows for homogeneous cell distribution with high viability within microgels, however, encapsulated cells in these polymers are typically unable to bind to the hydrogel limiting their utility in creating engineered tissues due to the inability of cells to remodel the surrounding environment [49]. The addition of binding motifs, either through incorporation of cell-adhesive peptide sequences [11,49–53] or mixing with native ECM components such as collagen I [19] or with other naturally derived proteins such as fibrin [54], improves cell binding and elongation. While there is the potential to include more specific binding motifs to encourage cell adhesion, in most synthetic hydrogel systems the binding motifs would only be linked to the ends of the polymer base, or to bridging linker proteins. One advantage of GelMA is the presence of binding sites distributed throughout the hydrogel on all polymer chains, potentially improving the probability of cell binding. Cells easily bound

to, and formed a monolayer on GelMA surfaces, and elongated and migrated within GelMA demonstrating its positive cell-binding behavior. However, all cell elongation and migration will be limited by the cell's ability to degrade and remodel the matrix which varies greatly among different cell types.

Synthetic hydrogels have been produced that contain both cell binding and cell-degrading motifs for use in tissue engineering and functional cell assays. Two major formulations have been presented which either incorporate RGD and MMP-sensitive regions on linker proteins which polymerize with 4-arm PEG using Michael-type addition [24,26,55,56], or by adding ECM degradation and binding sequences to the acrylate groups of PEG [52]. These hydrogels have been shown to encourage cell elongation, migration and interconnection *in vitro*, and cell infiltration and integration *in vivo*. However, both of these classes of hydrogels have potential disadvantages. For example, PEG hydrogels produced by Michael-type addition may be difficult to micropattern in comparison to photopolymerizable materials. Photopatterning of GelMA behaved similarly to photopatterned PEGDA in terms of UV exposure time, fidelity of micropatterns and ability to create and perfuse microchannels, however GelMA typically required either slightly shorter UV exposure or reduced photoinitiator concentrations. Therefore, GelMA could potentially be used in most microscale applications that photopolymerizable PEG has been demonstrated in, with similar, or better cell-responsive characteristics as PEG containing cell-binding and degradation motifs.

Overall we present evidence that GelMA would be suitable for a number of tissue engineering applications. For instance, GelMA allowed rapid cell adhesion, proliferation and migration on the surface of micropatterns. This could make GelMA well suited for controlled 2D cell interaction or cell shape studies by providing a rapid technique to create selectively binding regions of GelMA on PEG surfaces. In addition, encapsulated cells inside GelMA micropatterns elongated and reorganized. These data not only demonstrate that GelMA allows for cell migration, organization and interaction in both 2D and 3D, but also suggest that GelMA would be well suited for creating complex engineered tissues with features controllable on the microscale. For example, functional cells could be encapsulated in GelMA containing microchannels lined with endothelial cells to create microvascularized biomimetic tissues. Microvascular systems fabricated in a similar manner using collagen have been shown to support HUVEC attachment, spreading and function when externally perfused [57]. A GelMA-based system increases the mechanical stability of the gels as well as the ability to generate shape-controlled microgels relative to collagen. Finally, the ability to encourage cell-responsive behavior while enabling surface binding would make GelMA well suited for creating vascularized engineered tissues.

Conclusion

In this report we demonstrated the use of GelMA for microscale tissue engineering applications, highlighting the unique properties that make GelMA an attractive material for creating cell-laden microtissues. The physical properties of GelMA were demonstrated to be controllable through variation of the degree of methacrylation and the gel concentration yielding a tunable range of mechanical and swelling properties for different applications. GelMA was easily patterned down to 100 um resolution with the fidelity and robustness needed to perform as a cell-laden microgel or as a microfluidic device, similar to other commonly used hydrogels. However, unlike other synthetic UV crosslinkable hydrogels, cells readily adhered to, migrated within, proliferated and organized both in 2D and 3D in GelMA micropatterns. These data suggest that GelMA could be used for many microscale applications where other hydrogels are not well suited, such as for creating endothelial-lined vasculature within engineered tissues.

Acknowledgments

We thank Dr. Seung Hwan Lee for scientific discussions and Dr. Che Hutson, Jeff Simpson and Majid Ghodoosi for assistance with experiments. This paper was supported by the National Institutes of Health (DE019024; HL092836) and National Science Foundation (DMR0847287).

References

1. Khademhosseini A, Langer R, Borenstein J, Vacanti JP. Microscale technologies for tissue engineering and biology. Proc Natl Acad Sci U S A 2006;103(8):2480–2487. [PubMed: 16477028]
2. Chen CS, Mrksich M, Huang S, Whitesides GM, Ingber DE. Geometric control of cell life and death. Science 1997;276(5317):1425–1428. [PubMed: 9162012]
3. McBeath R, Pirone DM, Nelson CM, Bhadriraju K, Chen CS. Cell shape, cytoskeletal tension, and RhoA regulate stem cell lineage commitment. Dev Cell 2004;6(4):483–495. [PubMed: 15068789]
4. Nelson CM, Chen CS. Cell-cell signaling by direct contact increases cell proliferation via a PI3K-dependent signal. FEBS Lett 2002;514(2–3):238–242. [PubMed: 11943158]
5. Nelson CM, Liu WF, Chen CS. Manipulation of cell-cell adhesion using bowtie-shaped microwells. Methods Mol Biol 2007;370:1–10. [PubMed: 17416983]
6. Burdick JA, Vunjak-Novakovic G. Engineered microenvironments for controlled stem cell differentiation. Tissue Eng Part A 2009;15(2):205–219. [PubMed: 18694293]
7. Engler AJ, Sweeney HL, Discher DE, Schwarzbauer JE. Extracellular matrix elasticity directs stem cell differentiation. J Musculoskelet Neuronal Interact 2007;7(4):335. [PubMed: 18094500]
8. Engler AJ, Sen S, Sweeney HL, Discher DE. Matrix elasticity directs stem cell lineage specification. Cell 2006;126(4):677–689. [PubMed: 16923388]
9. Murtuza B, Nichol JW, Khademhosseini A. Micro- and nanoscale control of the cardiac stem cell niche for tissue fabrication. Tissue Eng Part B Rev 2009;15(4):443–454. [PubMed: 19552604]
10. Khademhosseini A, Vacanti JP, Langer R. Progress in tissue engineering. Sci Am 2009;300(5):64–71. [PubMed: 19438051]
11. Tsang VL, Chen AA, Cho LM, Jadin KD, Sah RL, DeLong S, West JL, Bhatia SN. Fabrication of 3D hepatic tissues by additive photopatterning of cellular hydrogels. FASEB J 2007;21(3):790–801. [PubMed: 17197384]
12. Nichol JW, Khademhosseini A. Modular tissue engineering: Engineering biological tissues from the bottom up. Soft Matter 2009;5:1312–1319. [PubMed: 20179781]
13. Dean DM, Napolitano AP, Youssef J, Morgan JR. Rods, tori, and honeycombs: The directed self-assembly of microtissues with prescribed microscale geometries. FASEB J 2007;21(14):4005–4012. [PubMed: 17627028]
14. Napolitano AP, Chai P, Dean DM, Morgan JR. Dynamics of the self-assembly of complex cellular aggregates on micromolded nonadhesive hydrogels. Tissue Eng 2007;13(8):2087–2094. [PubMed: 17518713]
15. Du Y, Lo E, Ali S, Khademhosseini A. Directed assembly of cell-laden microgels for fabrication of 3D tissue constructs. Proc Natl Acad Sci U S A 2008;105(28):9522–9527. [PubMed: 18599452]
16. McGuigan AP, Sefton MV. Vascularized organoid engineered by modular assembly enables blood perfusion. Proc Natl Acad Sci U S A 2006;103(31):11461–11466. [PubMed: 16864785]
17. Khademhosseini A, Eng G, Yeh J, Fukuda J, Blumling J III, Langer R, Burdick JA. Micromolding of photocrosslinkable hyaluronic acid for cell encapsulation and entrapment. J Biomed Mater Res A 2006;79(3):522–532. [PubMed: 16788972]
18. Yeh J, Ling Y, Karp JM, Gantz J, Chandawarkar A, Eng G, Blumling J III, Langer R, Khademhosseini A. Micromolding of shape-controlled, harvestable cell-laden hydrogels. Biomaterials 2006;27(31):5391–5398. [PubMed: 16828863]
19. Brigham MD, Bick A, Lo E, Bendali A, Burdick JA, Khademhosseini A. Mechanically robust and bioadhesive collagen and photocrosslinkable hyaluronic acid semi-interpenetrating networks. Tissue Eng Part A 2009;15(7):1645–1653. [PubMed: 19105604]

20. Yeo Y, Geng W, Ito T, Kohane DS, Burdick JA, Radisic M. Photocrosslinkable hydrogel for myocyte cell culture and injection. J Biomed Mater Res B Appl Biomater 2007;81(2):312–322. [PubMed: 16969828]
21. Yang F, Williams CG, Wang DA, Lee H, Manson PN, Elisseeff J. The effect of incorporating RGD adhesive peptide in polyethylene glycol diacrylate hydrogel on osteogenesis of bone marrow stromal cells. Biomaterials 2005;26(30):5991–5998. [PubMed: 15878198]
22. Ruoslahti E. RGD and other recognition sequences for integrins. Annu Rev Cell Dev Biol 1996;12:697–715. [PubMed: 8970741]
23. Benton JA, Fairbanks BD, Anseth KS. Characterization of valvular interstitial cell function in three dimensional matrix metalloproteinase degradable PEG hydrogels. Biomaterials 2009;30(34):6593–6603. [PubMed: 19747725]
24. Kraehenbuehl TP, Zammaretti P, Van der Vlies AJ, Schoenmakers RG, Lutolf MP, Jaconi ME, Hubbell JA. Three-dimensional extracellular matrix-directed cardioprogenitor differentiation: Systematic modulation of a synthetic cell-responsive PEG-hydrogel. Biomaterials 2008;29(18):2757–2766. [PubMed: 18396331]
25. Seliktar D, Zisch AH, Lutolf MP, Wrana JL, Hubbell JA. MMP-2 sensitive, VEGF-bearing bioactive hydrogels for promotion of vascular healing. J Biomed Mater Res A 2004;68(4):704–716. [PubMed: 14986325]
26. Lutolf MP, Weber FE, Schmoekel HG, Schense JC, Kohler T, Muller R, Hubbell JA. Repair of bone defects using synthetic mimetics of collagenous extracellular matrices. Nat Biotechnol 2003;21(5):513–518. [PubMed: 12704396]
27. Van Den Bulcke AI, Bogdanov B, De Rooze N, Schacht EH, Cornelissen M, Berghmans H. Structural and rheological properties of methacrylamide modified gelatin hydrogels. Biomacromolecules 2000;1(1):31–38. [PubMed: 11709840]
28. Galis ZS, Khatri JJ. Matrix metalloproteinases in vascular remodeling and atherogenesis: The good, the bad, and the ugly. Circ Res 2002;90(3):251–262. [PubMed: 11861412]
29. Van den Steen PE, Dubois B, Nelissen I, Rudd PM, Dwek RA, Opdenakker G. Biochemistry and molecular biology of gelatinase B or matrix metalloproteinase -9 (MMP-9). Crit Rev Biochem Mol Biol 2002;37(6):375–536. [PubMed: 12540195]
30. Benton JA, DeForest CA, Vivekanandan V, Anseth KS. Photocrosslinking of gelatin macromers to synthesize porous hydrogels that promote valvular interstitial cell function. Tissue Eng Part A 2009;15(11):3221–3230. [PubMed: 19374488]
31. Habeeb AF. Determination of free amino groups in proteins by trinitrobenzenesulfonic acid. Anal Biochem 1966;14(3):328–336. [PubMed: 4161471]
32. Brinkman WT, Nagapudi K, Thomas BS, Chaikof EL. Photo-cross-linking of type I collagen gels in the presence of smooth muscle cells: Mechanical properties, cell viability, and function. Biomacromolecules 2003;4(4):890–895. [PubMed: 12857069]
33. Podczeck, F.; Jones, B. Pharmaceutical capsules. RTJ, editor. London: The Pharmaceutical Press; 2004. p. 27
34. Peppas N, Hilt J, Khademhosseini A, Langer R. Hydrogels in biology and medicine: From molecular principles to bionanotechnology. Adv Mater 2006;18(11):1345–1360.
35. Lee KY, Mooney DJ. Hydrogels for tissue engineering. Chem Rev 2001;101(7):1869–1879. [PubMed: 11710233]
36. Tabata Y. Significance of release technology in tissue engineering. Drug Discov Today 2005;10(23–24):1639–1646. [PubMed: 16376824]
37. Kimura Y, Ozeki M, Inamoto T, Tabata Y. Adipose tissue engineering based on human preadipocytes combined with gelatin microspheres containing basic fibroblast growth factor. Biomaterials 2003;24(14):2513–2521. [PubMed: 12695078]
38. Dreesmann L, Ahlers M, Schlosshauer B. The pro-angiogenic characteristics of a cross-linked gelatin matrix. Biomaterials 2007;28(36):5536–5543. [PubMed: 17889331]
39. Kuijpers AJ, Engbers GHM, Feijen J, De Smedt SC, Meyvis TKL, Demeester J, Krijgsveld J, Zaat SAJ, Dankert J. Characterization of the network structure of carbodiimide cross-linked gelatin gels. Macromolecules 1999;32(10):3325–3333.

40. Saito H, Murabayashi S, Mitamura Y, Taguchi T. Characterization of alkali-treated collagen gels prepared by different crosslinkers. J Mater Sci Mater Med 2008;19(3):1297–1305. [PubMed: 17851737]
41. Choi YS, Hong SR, Lee YM, Song KW, Park MH, Nam YS. Studies on gelatin-containing artificial skin: II. Preparation and characterization of cross-linked gelatin-hyaluronate sponge. J Biomed Mater Res 1999;48(5):631–639. [PubMed: 10490676]
42. Choi YS, Hong SR, Lee YM, Song KW, Park MH, Nam YS. Study on gelatin-containing artificial skin: I. Preparation and characteristics of novel gelatin-alginate sponge. Biomaterials 1999;20(5): 409–417. [PubMed: 10204983]
43. Drury JL, Mooney DJ. Hydrogels for tissue engineering: Scaffold design variables and applications. Biomaterials 2003;24(24):4337–4351. [PubMed: 12922147]
44. Gendler E, Gendler S, Nimni ME. Toxic reactions evoked by glutaraldehyde-fixed pericardium and cardiac valve tissue bioprosthesis. J Biomed Mater Res 1984;18(7):727–736. [PubMed: 6085799]
45. Liang HC, Chang WH, Lin KJ, Sung HW. Genipin-crosslinked gelatin microspheres as a drug carrier for intramuscular administration: In vitro and in vivo studies. J Biomed Mater Res A 2003;65(2): 271–282. [PubMed: 12734822]
46. Barker H, Oliver R, Grant R, Stephen L. Formaldehyde as a pre-treatment for dermal collagen heterografts. Biochim Biophys Acta 1980;632(4):589–597. [PubMed: 6254577]
47. Broderick EP, O'Halloran DM, Rochev YA, Griffin M, Collighan RJ, Pandit AS. Enzymatic stabilization of gelatin-based scaffolds. J Biomed Mater Res B Appl Biomater 2005;72(1):37–42. [PubMed: 15490480]
48. Crescenzi V, Francescangeli A, Taglienti A. New gelatin-based hydrogels via enzymatic networking. Biomacromolecules 2002;3(6):1384–1391. [PubMed: 12425680]
49. Mann BK, West JL. Cell adhesion peptides alter smooth muscle cell adhesion, proliferation, migration, and matrix protein synthesis on modified surfaces and in polymer scaffolds. J Biomed Mater Res 2002;60(1):86–93. [PubMed: 11835163]
50. Schmedlen RH, Masters KS, West JL. Photocrosslinkable polyvinyl alcohol hydrogels that can be modified with cell adhesion peptides for use in tissue engineering. Biomaterials 2002;23(22):4325–4332. [PubMed: 12219822]
51. Mann BK, Tsai AT, Scott-Burden T, West JL. Modification of surfaces with cell adhesion peptides alters extracellular matrix deposition. Biomaterials 1999;20(23–24):2281–2286. [PubMed: 10614934]
52. Mann BK, Gobin AS, Tsai AT, Schmedlen RH, West JL. Smooth muscle cell growth in photopolymerized hydrogels with cell adhesive and proteolytically degradable domains: Synthetic ECM analogs for tissue engineering. Biomaterials 2001;22(22):3045–3051. [PubMed: 11575479]
53. Gobin AS, West JL. Cell migration through defined, synthetic ECM analogs. FASEB J 2002;16(7): 751–753. [PubMed: 11923220]
54. Dikovsky D, Bianco-Peled H, Seliktar D. The effect of structural alterations of PEG-fibrinogen hydrogel scaffolds on 3-D cellular morphology and cellular migration. Biomaterials 2006;27(8): 1496–1506. [PubMed: 16243393]
55. Raeber GP, Lutolf MP, Hubbell JA. Molecularly engineered PEG hydrogels: A novel model system for proteolytically mediated cell migration. Biophys J 2005;89(2):1374–1388. [PubMed: 15923238]
56. Lutolf MP, Lauer-Fields JL, Schmoekel HG, Metters AT, Weber FE, Fields GB, Hubbell JA. Synthetic matrix metalloproteinase-sensitive hydrogels for the conduction of tissue regeneration: Engineering cell-invasion characteristics. Proc Natl Acad Sci U S A 2003;100(9):5413–5418. [PubMed: 12686696]
57. Chrobak KM, Potter DR, Tien J. Formation of perfused, functional microvascular tubes in vitro. Microvasc Res 2006;71(3):185–196. [PubMed: 16600313]

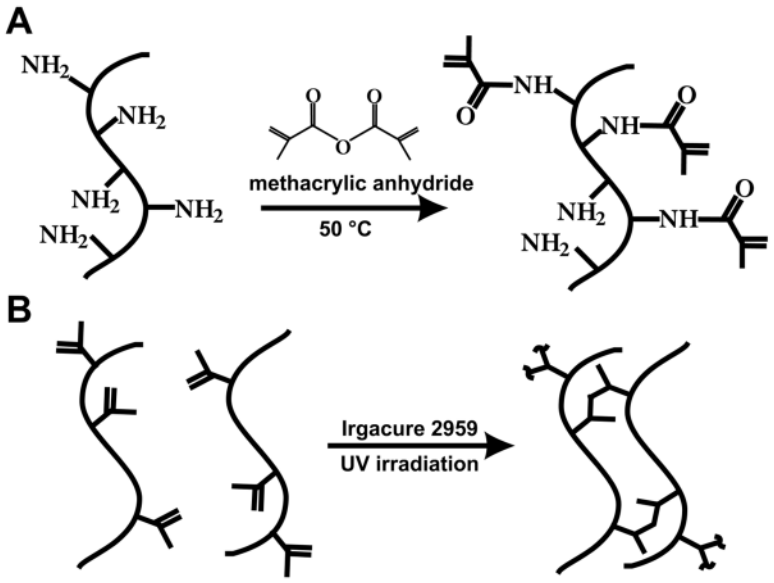

Figure 1.
Synthesis of methacrylated gelatin. Gelatin macromers containing primary amino groups were reacted with methacrylic anhydride (MA) to add methacrylate pendant groups (A). To create a hydrogel network, the methacrylated gelatin (GelMA) was crosslinked using UV irradiation in the presence of a photoinitiator (B).

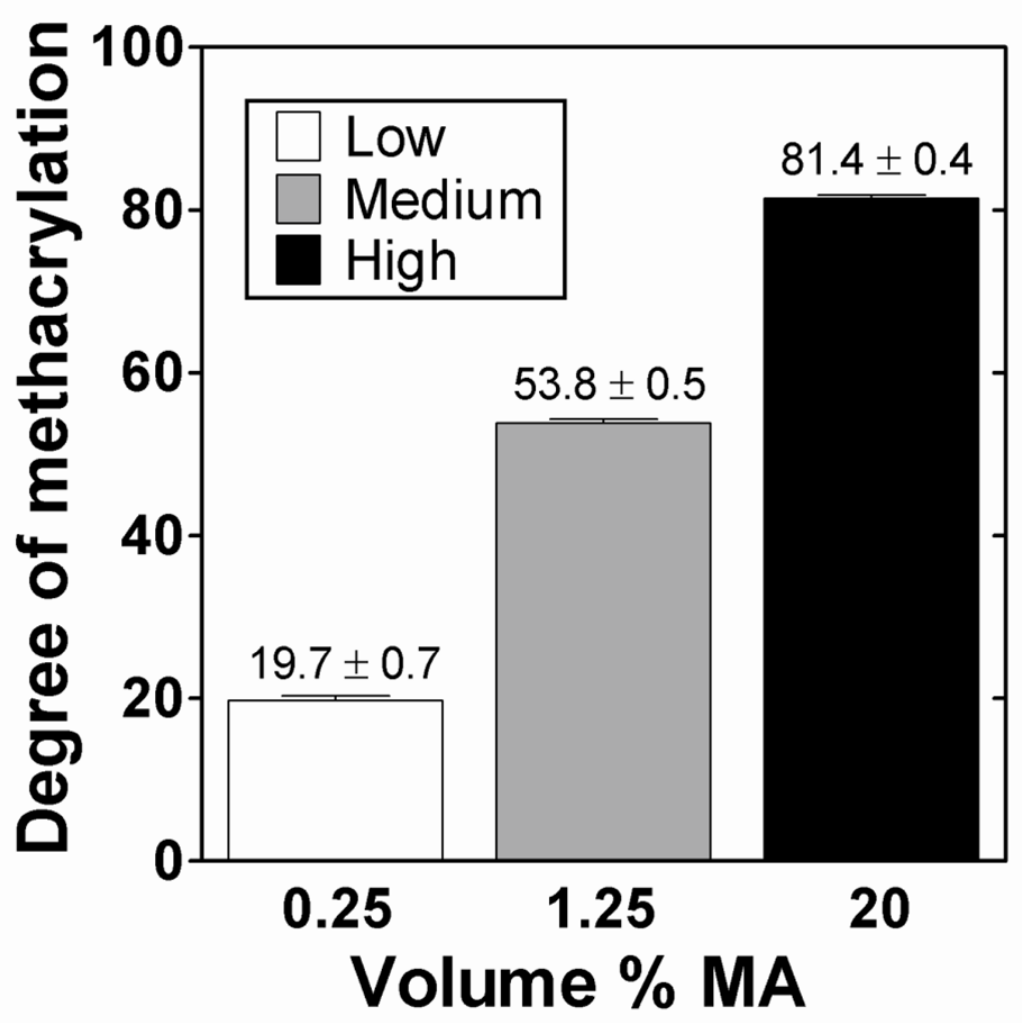

Figure 2.
Degree of methacrylation as determined by ^{1}H-NMR. The degree of methacrylation was determined for various methacrylic anhydride volume percentages present in the synthesis reaction. The percentage of methacrylate groups incorporated was determined by comparing the integrated intensity of the double bond peak to that of the aromatic side chains. Error bars represent the SD of 3 repeated measurements on each sample.

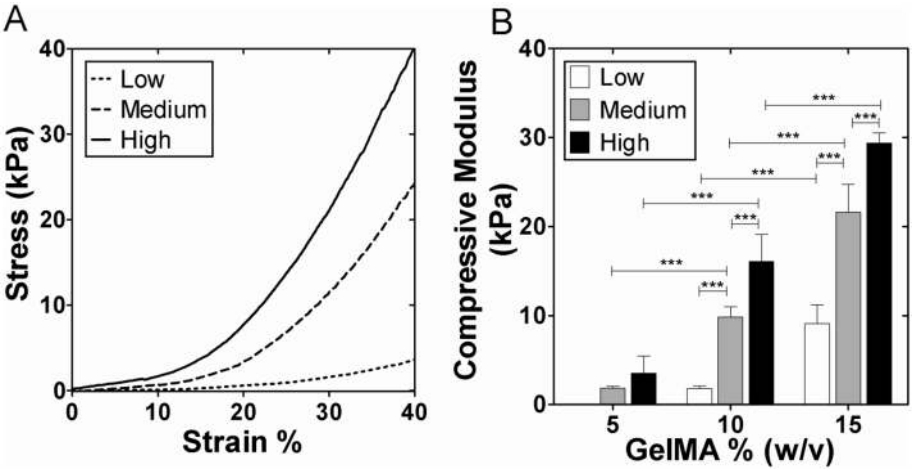

Figure 3.

Mechanical properties of GelMA with varying gel percentage and degree of methacrylation. Representative curves from 15% GelMA at varying degree of methacrylation (A). Compressive modulus for 5%, 10% and 15% (w/v) GelMA at low, medium and high degree of methacrylation (B), with the exception of low degree, 5% (w/v) GelMA which formed gels which were too weak to be handled for testing. All conditions were significantly different (***$p < 0.001$) except with 5% (w/v) GelMA. Error bars represent the SD of measurements performed on 5 samples.

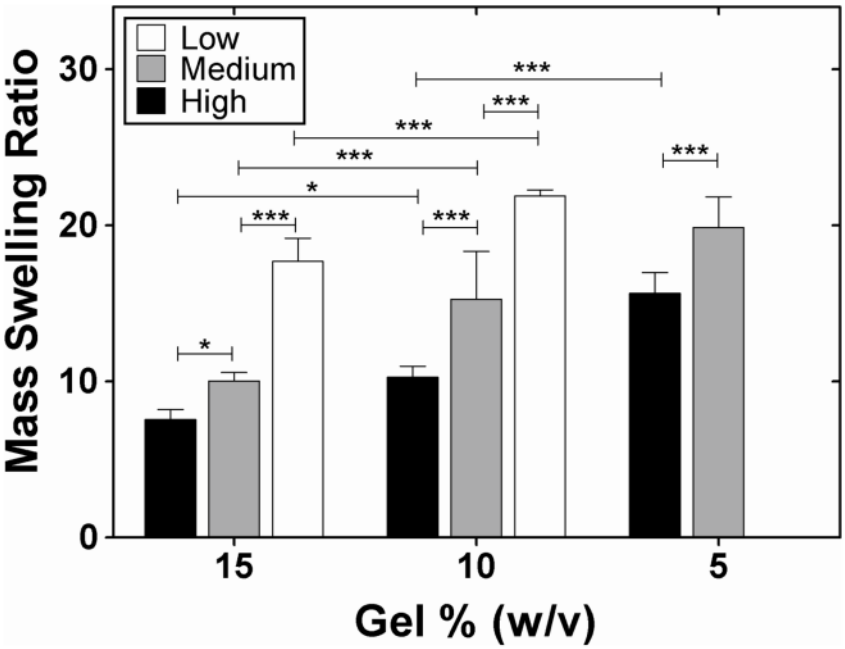

Figure 4.

Equilibrium swelling properties of methacrylated gelatin hydrogels. The mass swelling ratios of GelMA hydrogels at various GelMA % (w/v) and degrees of methacrylation show statistically significant differences (*p<0.05, **p<0.01, ***p<0.001). Low methacrylation GelMA formed gels which were too weak to be handled at 5% (w/v) concentration and were not studied. Error bars represent the SD of measurements performed on at least 3 samples.

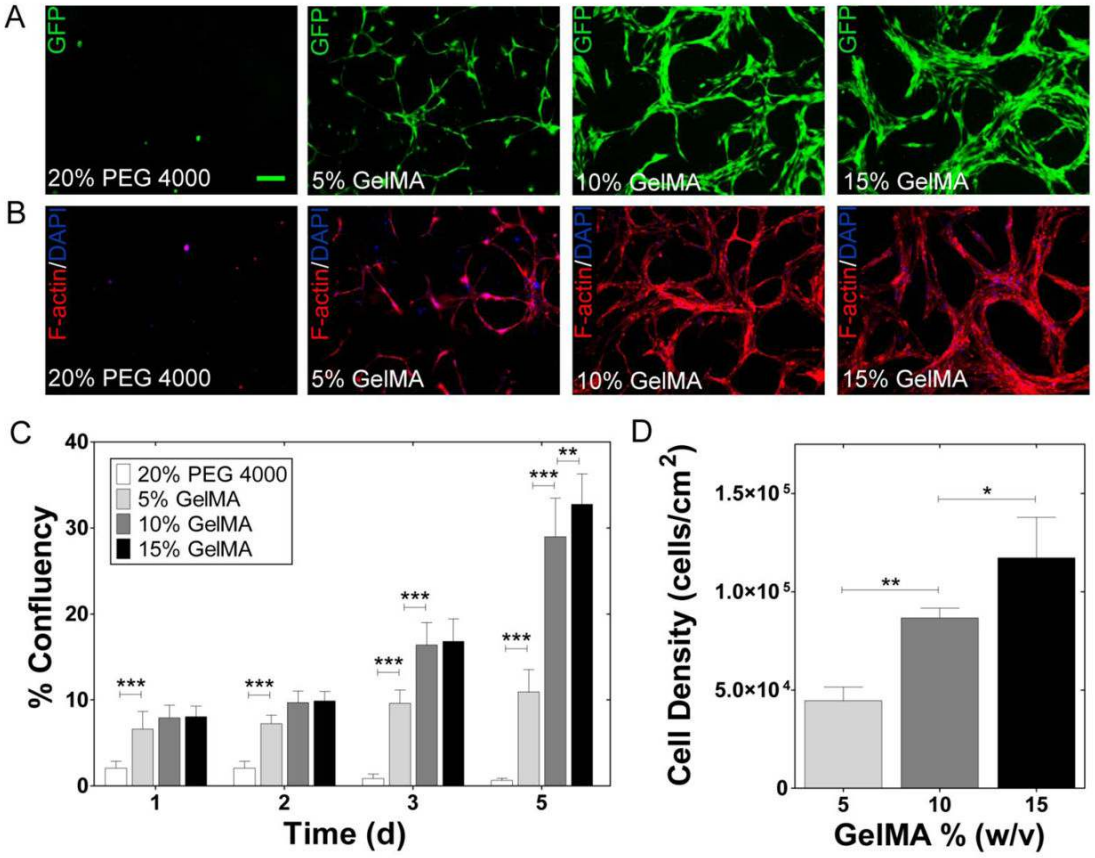

Figure 5.

Cell adhesion, proliferation and migration on GelMA surfaces. HUVEC cells readily adhered to GelMA of all macromer concentrations, but did not adhere to PEG 4000 as demonstrated by endogenous GFP (A) and rhodamine-labeled phalloidin/DAPI staining for F-actin/cell nuclei (B) on day 5 of culture (scale bar = 200 μm). While initial binding was similar regardless of GelMA hydrogel percentage, over time confluency was significantly different proportional to the hydrogel percentage (*p<0.05,**p<0.01,***p<0.001) (C). Determination of cell density, defined as the number of DAPI stained nuclei per given hydrogel area, demonstrated a similar, significant relationship between cell number and GelMA percentage consistent with total confluency (D). Error bars represent the SD of averages obtained on 3 images from each of 6 independent samples per condition.

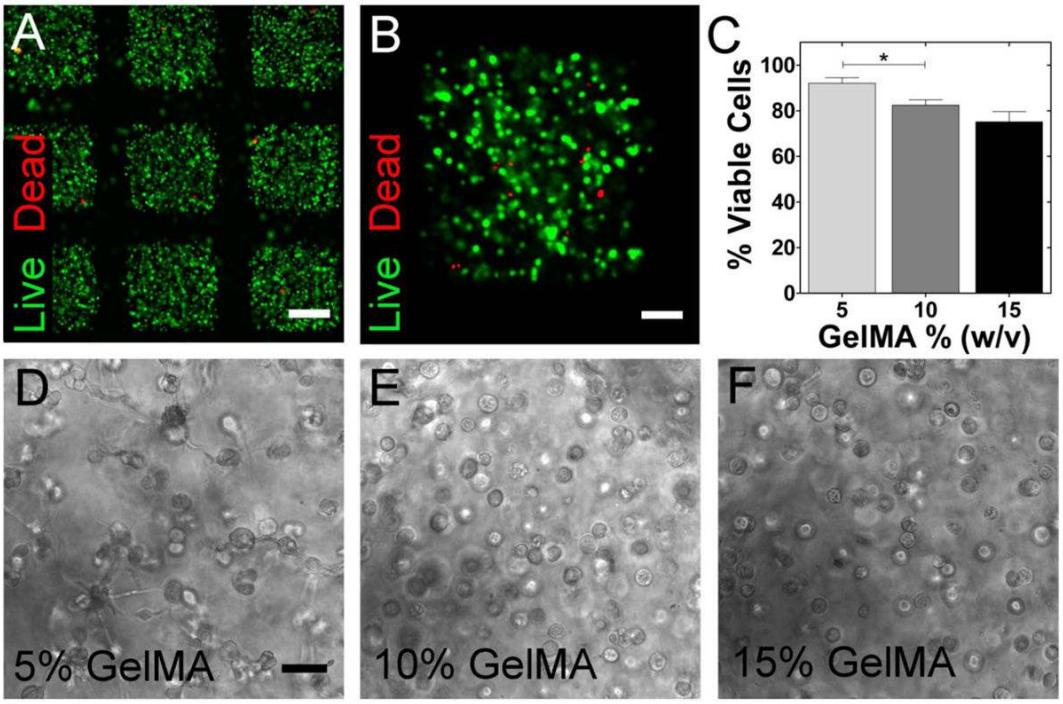

Figure 6.

Characterization of embedded cell behavior in micropatterned GelMA. 3T3 fibroblasts embedded in GelMA micropatterns of various macromer concentration were stained with calcein-AM (green)/ethidium homodimer (red) LIVE/DEAD assay 8 h after encapsulation shown at low (scale bar = 250 μm) (A) and high (scale bar = 100 μm) magnification (B). Quantification of cell viability demonstrated excellent cell survival at all conditions (*$p<0.05$) (C). After 2 days in culture, cells were seen to elongate and form interconnected networks in GelMA inversely proportional to the hydrogel concentration (scale bar = 50 μm) (D–F). Error bars represent the SD of 3 independent samples.

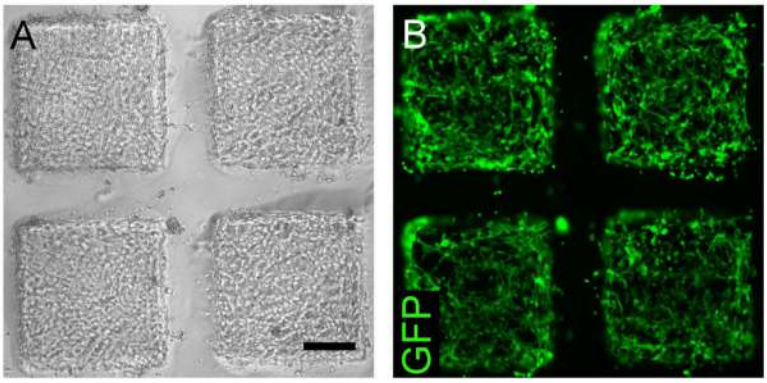

Figure 7.
Selective binding to GelMA micropatterns. GelMA micropatterns were photopolymerized on a prefabricated PEG-coated glass slide. GFP-expressing HUVEC cells seeded on this composite array bound only to the GelMA surfaces, quickly forming confluent monolayers (scale bar = 200 μm) (A,B).

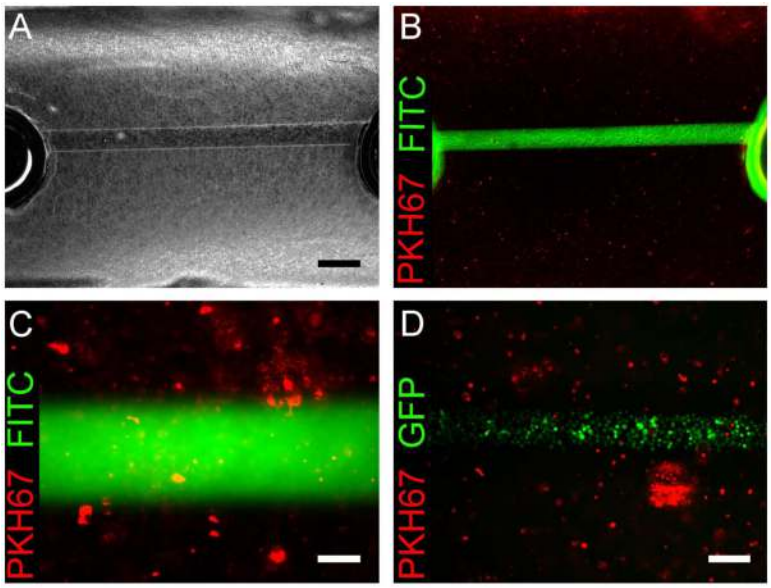

Figure 8.
Microfluidic channels and cell seeding in cell-laden GelMA. Microfluidic channels that were 300 μm in diameter (scale bar = 500 μm) (A), were created in GelMA containing PKH67 labeled 3T3 fibroblasts, allowing for perfusion visualized by FITC-Dextran (2000 kDa) as shown at low (B) and high magnification (scale bar = 100 μm) (C). Seeding of GFP-HUVEC cells in cell-laden GelMA allowed for attachment, demonstrating the ability to create cell-laden microgels with endothelial-lined, perfusable microvasculature (scale bar = 200 μm) (D).